Improved Hybrid Solar Cells via in situ UV Polymerization

Sanja Tepavcevic, Seth B. Darling, Nada M. Dimitrijevic, Tijana Rajh, and Steven J. Sibener*

One approach for making inexpensive inorganic–organic hybrid photovoltaic (PV) cells is to fill highly ordered TiO_2 nanotube (NT) arrays with solid organic hole conductors such as conjugated polymers. Here, a new in situ UV polymerization method for growing polythiophene (UV-PT) inside TiO_2 NTs is presented and compared to the conventional approach of infiltrating NTs with pre-synthesized polymer. A nanotubular TiO_2 substrate is immersed in a 2,5-diiodothiophene (DIT) monomer precursor solution and then irradiated with UV light. The selective UV photodissociation of the C–I bond produces monomer radicals with intact π-ring structure that further produce longer oligothiophene/PT molecules. Complete photoluminescence quenching upon UV irradiation suggests coupling between radicals created from DIT and at the TiO_2 surface via a charge transfer complex. Coupling with the TiO_2 surface improves UV-PT crystallinity and π–π stacking; flat photocurrent values show that charge recombination during hole transport through the polymer is negligible. A non-ideal, backside-illuminated setup under illumination of 620-nm light yields a photocurrent density of $\approx 5\ \mu A\ cm^2$ — surprisingly much stronger than with comparable devices fabricated with polymer synthesized ex situ. Since in this backside architecture setup we illuminate the cell through the Ag top electrode, there is a possibility for Ag plasmon-enhanced solar energy conversion. By using this simple in situ UV polymerization method that couples the conjugated polymer to the TiO_2 surface, the absorption of sunlight can be improved and the charge carrier mobility of the photoactive layer can be enhanced.

Keywords:
- conducting polymers
- nanotubes
- photoconductivity
- self-assembly
- solar cells

1. Introduction

Hybrid solar cells have been developed in the past decade as a promising alternative for traditional Si-based solar cells. A wide-bandgap metal oxide like TiO_2, sensitized by an organic semiconductor, dye molecule, or quantum dots,[1–6] offers the promise of low-cost, large-area conversion of solar energy to electricity. The nanoscale morphology of such devices is crucial for their performance: a simple layered (planar heterojunction) donor–acceptor device structure yields cells with poor efficiency due to limited interfacial area, charge carrier recombination, and overly thin layers necessitated by exciton diffusion distances (5–20 nm).[7] Enlargement of the interfacial area is accomplished in dye-sensitized solar cells, in which a highly porous film of TiO_2 nanoparticles is covered with a monolayer of a metal-organic sensitizer that absorbs

[*] Dr. S. B. Darling, Dr. N. M. Dimitrijevic, Dr. T. Rajh
Argonne National Laboratory
Center for Nanoscale Materials
9700 S Cass Ave, Argonne, IL 60439 (USA)
E-mail: darling@anl.gov
Dr. S. Tepavcevic, Prof. S. J. Sibener
Department of Chemistry, The James Franck Institute
The University of Chicago
929 E 57th St, Chicago, IL 60637 (USA)
Dr. N. M. Dimitrijevic
Argonne National Laboratory
Chemical Sciences and Engineering Division
9700 S Cass Ave, Argonne, IL 60439 (USA)

Supporting Information is available on the WWW under http://www.small-journal.com or from the author.

DOI: 10.1002/smll.200900093

NANO MICRO small

visible light.[5] Although energy conversion efficiencies can exceed 10%, the necessity of a liquid electrolyte to accomplish regeneration of the oxidized dye calls for elaborate sealing techniques, which has hindered commercialization thus far. Conventional bulk heterojunction (BHJ) solar cells consist of a randomly structured contact between the donor and acceptor layers; limitations of this disordered configuration include non-ideal domain length scales, charge trapping at bottlenecks, and dead-ends in the conducting pathways to the electrodes.[7,8] In contrast, highly ordered, vertically oriented, crystalline TiO_2 nanotube (NT) arrays fabricated by potentiostatic anodization provide good pathways for electron migration through the active layer.[9] This nanomaterial provides substantial surface area while maintaining a highly ordered structure.[10] Furthermore, this architecture offers the ability to influence the absorption and propagation of light through the architecture by precisely designing and controlling the architectural parameters including NT pore size, wall thickness, and length.[11–13]

One approach for making inexpensive inorganic–organic hybrid photovoltaic (PV) cells is to fill nanostructured titania films with solid organic-hole conductors such as conjugated polymers.[9] These compounds can function as light-absorbing species and inject electrons into the conduction band of the n-type semiconductor, while at the same time they conduct the holes to the cathode. Oligothiophenes and polythiophenes (PTs), in particular, have strong potential in the fields of electronics, sensors, solar cells, and displays because of their superior thermal and environmental stability as well as their interesting electronic properties. One of the more heavily investigated PTs is poly(3-hexylthiophene) (P3HT) due to its large absorption coefficient (close to the maximum photon flux in the solar spectrum) and its high hole mobility of 0.1 $cm^2 Vs^{-1}$ in its ordered, regioregular form, which is among the highest for polymeric semiconductors.[1,9,11]

NT films offer a distinct advantage over nanoparticle films in that they facilitate charge carrier transport. The electrons in particulate TiO_2 films are more susceptible to loss at grain boundaries than those in NT TiO_2 films.[6] One also needs to take into consideration the relative roles of crystal structure and surface defects comparing TiO_2 tubes and particles in the context of their interaction with polymers. In addition to the improved electron mobility associated with ordered metal oxide nanostructures, the hole mobility of the conjugated polymer may be enhanced in the direction normal to the substrate by infiltrating the polymer into a NT architecture as a result of alignment of the polymer chains along the walls of the pores.[12] Compared to the more commonly used ruthenium-based dyes, conjugated polymers are relatively inexpensive as sensitizers. In films sensitized by molecular dyes, the thickness of the nanostructured TiO_2 film needs to be at least 10 μm to harvest the maximal amount of incident photons, whereas for a polymer with a high absorption coefficient such as P3HT, a film several hundred nanometers in thickness is sufficient to optimally harvest incident sunlight. Thinner films translate into shorter pathways for the charge carriers and, hence, less non-geminate recombination.

The infiltration of the polymer into the nanostructured metal oxide is of particular importance for optimizing the performance of these hybrid devices.[14] Most of the reports on solar cells using conjugated polymers have employed wet processing deposition techniques such as spin-coating, dip-coating, drop-casting, doctor-blading, inkjet-printing, and screen-printing.[1–3] Since polymers suffer a loss of conformational entropy when they are confined in a channel whose radius is less than their radius of gyration, filling the pores with a polymer has been thought to be a challenge due to the possibility of the polymer chains clogging the pores of the nanotubular electrode.[9] Infiltration can be enhanced with melt processing, which has been connected to improved device performance.[15] Another approach is to chemically modify the surface of the oxide to create a more favorable surface energy, such as by incorporating phosphonic acid[16] or amine[17] moieties into molecular monolayers. Instead of using pre-synthesized polymer, one can attempt to circumvent this obstacle by producing oligothiophenes and PTs directly within nanostructured architectures. The electrochemical method is widely used to produce highly conducting PT thin films.[18] This method requires the use of conductive substrates and electrolyte solutions, which is not necessarily a drawback for PV applications. However, because this method initiates the polymerization at the electrode and not at the oxide surface, it does not address the poor coupling between the oxide and the polymer that affects most infiltration approaches. Solventless direct deposition approaches such as plasma polymerization, laser-induced chemical vapor deposition, as well as X-rays, electrons, and ion-induced synthesis in ultra-high vacuum (UHV) conditions have also been investigated.[19] However, these approaches, in general, do not have enough reaction specificity to generate reactive species without fragmentation of the monomer structure, which results in defect incorporation in the final product.

In this paper, we present a new technique for deposition/infiltration of conjugated polymers into densely ordered TiO_2 NT arrays. In particular, we report the effects of in situ UV polymerization of PT versus infiltration of pre-synthesized P3HT on the performance of solar cell devices. In our simple and efficient photochemical approach, a nanotubular TiO_2 substrate is immersed overnight in a 2,5-diiodothiophene (DIT) monomer precursor solution and then irradiated with UV light in an argon environment (see Supporting Information). The selective UV photodissociation of the C–I bond ($\lambda = 250$–300 nm) in the precursor molecule produces monomer radicals with intact π-ring structure. Since the C–I bonds are present at the ends of the reaction coupling products, further photodissociation can take place, forming oligomeric and polymer species that can couple to and self-assemble on the surface of TiO_2 NTs.[20] The formation of polymeric semiconductor films by this method offers distinct advantages such as cost, uniformity, and scalability over other solution processing techniques.

2. Results and Discussion

2.1. Fabrication of Hybrid Solar Cells

Vertically oriented crystalline TiO_2 NT arrays were prepared on transparent conducting substrates (Scheme 1).

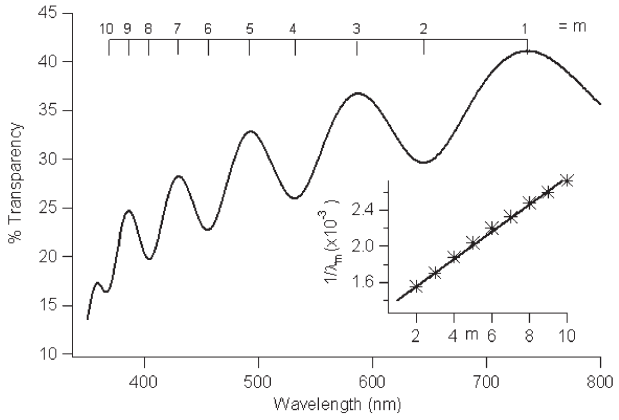

Figure 1. Typical fringe pattern of the transmission spectrum of a thin TiO_2 film on ITO surrounded by non-absorbing media measured against ITO.

The resulting length of the NTs (thickness of TiO_2 layer) can be estimated from the position of interference fringes present in transmission spectra (Figure 1) due to multiple reflections on the interfaces between media with different thicknesses and refractive indices. Equation 1 gives the dependence of the reciprocal value of the wavelengths ($1/\lambda_m$) on the order (m) of extremes (maxima and minima) in transmittance from longer to shorter wavelengths:[21]

$$\frac{1}{\lambda_m} = m\left(\frac{1}{4dn}\right) \quad (1)$$

where d is the thickness of the film in nm and n is the refractive index of TiO_2. Using an average value for the refractive index of the TiO_2 anatase crystal structure, $n = 2.52$,[22] we obtain the value of $d = 660$ nm from the slope of the data displayed in the Figure 1 inset. The resulting NT arrays had an average inner diameter of 30 nm and wall thickness of 5 nm (Figure 2 inset), which, importantly, is similar to the exciton diffusion distance in organic semiconductors. PV devices constructed with either in situ polymerized PT or P3HT were completed as depicted in Scheme 1 and as described later.

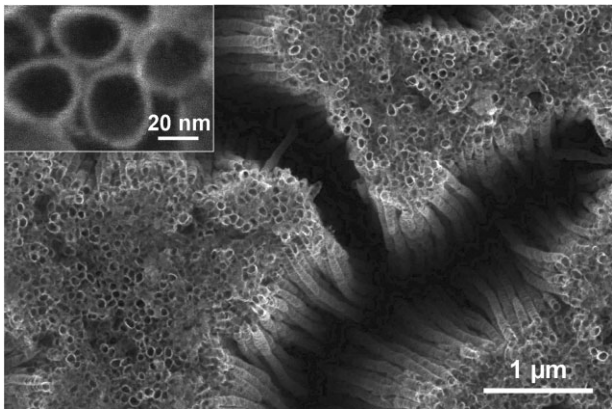

Figure 2. FESEM images of the TiO_2 NT array top surface after annealing. Inset shows a zoomed view of the NTs with 30-nm inner diameter and wall thickness of 5 nm.

2.2. In situ UV Polymerization and Coupling with the TiO_2 NT Surface

For creating high-quality conjugated polymers for PV devices, it is critical to minimize defects such as fragmented monomer structure, mislinking of monomer units (α–β and β–β coupling), conformational disorder,[23,24] and crosslinking of polymer chains. It has been demonstrated previously that in situ polymerization can be used to produce covalently surface-grafted regiorandom conjugated PT inside TiO_2 NTs.[25] In this method, P3HT was synthesized directly from the initiator group using 3HT as the monomer and $FeCl_3$ as a chemical oxidant. The organic monolayer bound on the titania surface containing thiophene moieties was used to initiate in situ polymerization. Surface-initiated in situ polymerization achieved better interface contact, larger surface coverage, and more complete filling compared with a nanoporous structure infiltrated by polymer synthesized outside the network. However, this methodology created regiorandom PT.

In contrast, by using in situ UV polymerization, monomer units preferentially connect via α–α coupling; upon absorption of UV photons, C–I bonds of the DIT precursor molecule selectively dissociate into a thienyl radical and iodine atoms. The excess kinetic energy imparted to the photogenerated radicals will be rapidly quenched via collisions in the condensed phase. During this collision process, some photogenerated radicals may react with unreacted monomers, making dimers that can be further activated by photons and involved in reactions forming oligomers and polymers, which we denote as UV-PT. Oxygenated defects are avoided by using an inert argon environment (water adsorption on the substrate is negligible at room temperature). By growing PT inside TiO_2 NTs, as opposed to infiltrating with polymer, we achieve more complete filling of the NTs due to the fact that it is much easier for the small molecule monomer to penetrate into the full volume of the NTs. Furthermore, because TiO_2 absorbs UV light so efficiently, the oxide NT network will serve as the primary conduit for the light energy to find its way to the precursor molecules. Because the UV light will come preferentially through the TiO_2, coupling between the resulting polymer and the oxide surface is promoted. One might think that polymer could be achieved more easily by starting with larger precursors, but this is, in fact, disadvantageous. It has been shown that when the starting molecules for UV polymerization are bithiophene or trithiophene, the corresponding decrease in orientational freedom of the molecules has a negative effect on the ease of polymerization and the structural order of the product.[26]

Figure 3 shows attenuated total reflection Fourier transform infrared (ATR-FTIR) spectra of pre-synthesized P3HT and photochemically synthesized PT infiltrated in TiO_2 NTs.[18] The peaks around 825 and 1052 cm^{-1} are associated with the δ_{CH} out-of-plane bending vibration and the δ_{CH} in-plane bending vibration, respectively, while the peaks around 2900–3100 cm^{-1} are assigned to the ν_{CH} stretching vibrations. The lower energy peaks are aliphatic and, in the case of the UV-PT, likely originate from some minor decomposition products. The highest energy of these peaks, associated with the 3 and 4 positions of the thiophene ring, indicates that the

small NANO MICRO

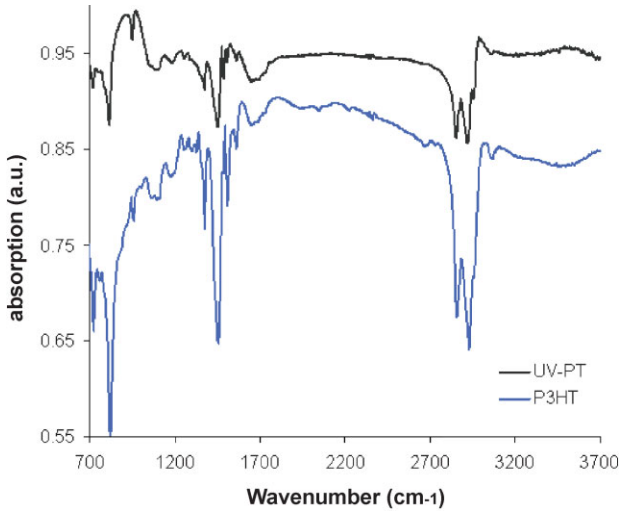

Figure 3. ATR-FTIR spectra of UV-PT and P3HT on TiO_2/ITO substrate. UV-PT was prepared by immersion of TiO_2 NTs in DIT monomer solution overnight prior to 15 min of UV irradiation. P3HT was prepared by drop-casting a polymer solution into TiO_2 NTs.

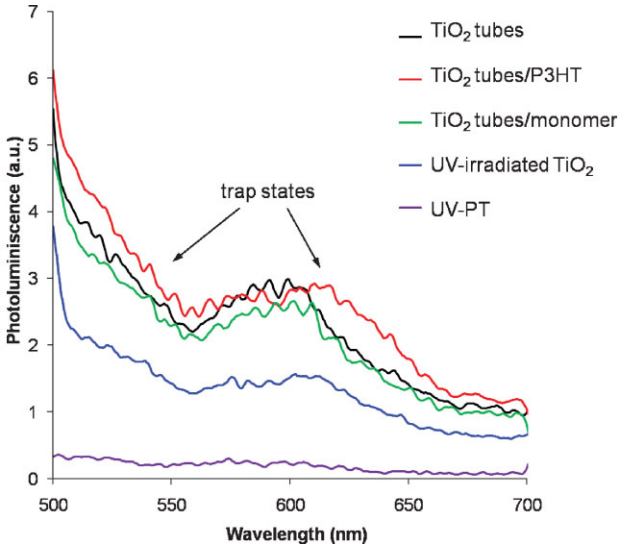

Figure 4. PL spectra of TiO_2 surface state trapping site quenching upon in situ UV polymerization. The conventional P3HT/TiO_2 system displays virtually no quenching. Excitation wavelength is 435 nm in all cases.

thiophene ring structure is intact upon photodissociation of the C–I bond and that the coupling reactions occur at the α positions from the sulfur atom. The single band at 1510 cm^{-1} is due to the C–C asymmetric (ν_{as}) stretching vibration, which is observed in a narrow region of 1530–1502 cm^{-1} for oligothiophenes and PTs. The peak at 1450 cm^{-1} and a shoulder at the lower wavelength side are attributed to the C=C symmetric (ν_s) stretching vibration. This peak position is very sensitive to the conjugation length in α–α'-coupled oligothiophenes. The C=C symmetric stretching band shifts to higher wavenumber with increasing conjugation length. The intensity ratio of symmetric and antisymmetric peaks ($I_{asym}/I_{sym} \approx 0.3$) and the location of the C=C symmetric stretching vibration peak of the UV produced film compared with those of P3HT indicate that the photosynthesized polymer film has a similar conjugation length distribution (at least eight conjugated thiophene ring units).[20] The FTIR spectrum of the photochemically synthesized film shows no peak in the 1650–1750 cm^{-1} region, indicating that oxidation defects and contamination are relatively small (the small peaks at 1090 and 1190 cm^{-1} are indicative of some oxidative doping[27]). Moreover, the ATR-FTIR spectra contain evidence for coupling of UV-polymerized thiophene to the TiO_2 surface: disappearance of a broad absorption band at around 3400 cm^{-1}, assigned to the stretching vibrations of O–H groups, and appearance of new peaks in the 2000–2350 cm^{-1} range suggest structural changes in TiO_2 due to photoinduced interaction with the polymer.

Photoluminescence (PL) spectra (excitation wavelength of 435 nm) in Figure 4 show luminescence from surface trap states[28] present on the TiO_2 NTs prior to and after infiltration of the DIT monomer or P3HT. Upon UV irradiation of TiO_2 NTs we observe a decrease in the intensity of the luminescence centered at 617 nm, attributed to oxygen vacancies (intergap surface states) due to radical trapping on the TiO_2 surface. After 15 min in the dark, these radicals recombine and UV-irradiated TiO_2 shows the same spectra as pre-irradiated TiO_2 tubes (Figure 5). However, upon UV irradiation of TiO_2 NTs infiltrated with monomer precursor complete and irreversible

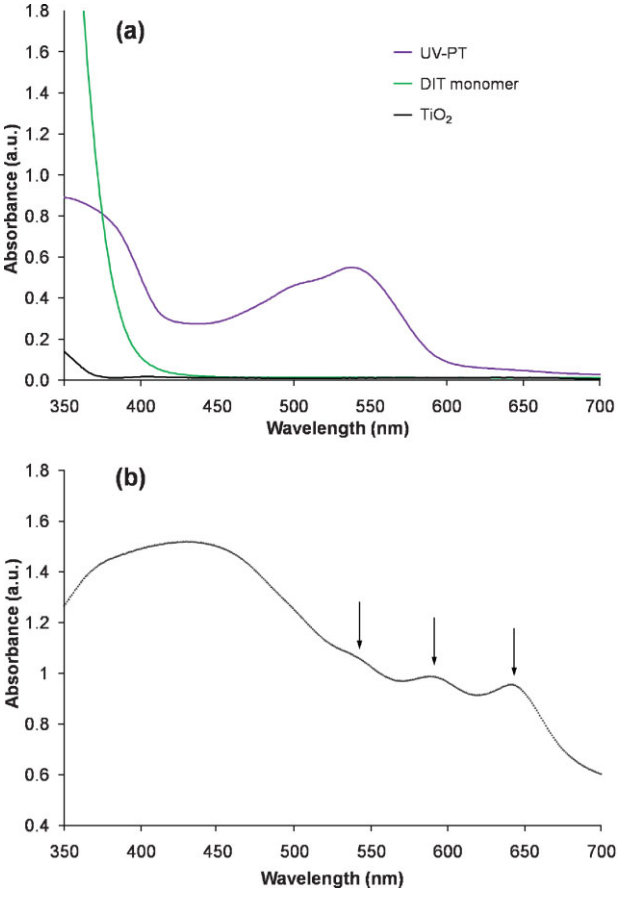

Figure 5. Absorption spectra of UV-PT (after 15 min of UV irradiation) and DIT monomer on glass (a) compared with TiO_2 and the solar spectrum and UV-PT on ITO/TiO_2 (b).

PL quenching is observed. This result indicates an excited-state interaction between the two semiconductor materials and deactivation of the excited PT via electron transfer to TiO_2. Such quenching behavior suggests electronic coupling between the TiO_2 surface and DIT via a charge transfer complex. The inability of the infiltrated P3HT to similarly quench PL indicates limitations to charge transfer processes at the TiO_2/polymer interface, which could result in decreased exciton separation effectiveness. Moreover, UV-PT has a characteristic PL emission centered near 550 nm when excited at 435 nm[19] that is also quenched in this hybrid system. The efficiency of charge transfer between the polymer and the titania is greatly enhanced using in situ polymerization.

Further evidence of coupling between in situ polymerized PT and the TiO_2 NT surface is a qualitative difference in the absorption spectra of polymer on glass (Figure 5a) and on the TiO_2 surface (Figure 5b). The absorption spectra of the UV-polymerized film on glass show signatures of oligothiophenes (peak near 500 nm) and PTs (peak at 545 nm).[29] Analysis can be facilitated by comparison to data from ordered aggregates of P3HT in solution, for which the main π–π* absorption band is at 515 nm and two vibronic absorption shoulders are at 558 and 607 nm. The vibronic shoulder peak at 558 nm is attributed to absorptions of extended conjugation lengths resulting from the ordered packing of P3HT backbones, whereas the peak at 607 nm originates from a transition between P3HT chains, whose intensity reflects the quality of chain packing.[30] Due to coupling with the TiO_2 surface and improved UV-PT crystallinity and π–π stacking relative to the polymer on a glass substrate, the absorption spectra of the monomer polymerized inside TiO_2 NTs show vibronic signatures similar to that of ordered aggregates (Figure 5b). Interestingly, there is an additional red-shifted peak around 640 nm (see arrow), which is redder than any known absorption from P3HT. The origin of this peak is currently not known, but it may be due to some branching of the PT chains since aromatic side groups are capable of red shifting absorption spectra. This peak could be technologically important because it enables the system to capture some longer wavelength photons that would not have sufficient energy to create excitons in a typical P3HT device. When the monomer precursor was UV-polymerized on a glass substrate (Figure 5a), that is, with no TiO_2 present, the two vibronic absorption peaks are not resolved, suggesting that the crystallinity and π–π stacking of UV-PT is lower in the absence of TiO_2. Low crystalline order has been demonstrated to be one of the foremost obstacles to achieving high performance devices based on crystallizable polymer. By using this simple in situ UV polymerization method that couples polymer to the TiO_2 surface and creates longer and interconnected oligothiophene/PT molecules, one aims to improve absorption of sunlight and enhance charge carrier mobility of the photoactive layer.

2.3. Solar-Cell Performance

Ideally, the TiO_2 NT depth would be engineered to be slightly smaller than the initial Ti layer thickness, rendering this part of the device transparent and hence enabling front side illumination (Scheme 1). Due to the 300-nm-thick layer of Ti still present between indium tin oxide (ITO) and the TiO_2 NT layer in our device, standard front-side device illumination was not possible. In order to achieve a photoelectrochemical response, the ITO/Ti/TiO_2(NT)/UV-PT/Ag architecture was illuminated from the backside through the 30-nm-thick Ag top electrode. The thickness of the Ag film was optimized to balance the need for optical transmittance and electrical conductivity.[31] In the range from 350 to 700 nm, transmittance of the 30-nm-thick Ag top electrode varies from 55% (350 nm) down to <10% (700 nm). This type of device acts as a solid state non-electrochemical version of dye-sensitized Grätzel cells: the anode and the cathode serve only as quasi-Ohmic contacts and the internal field originates from the difference between the Fermi level of the TiO_2 and the HOMO of the conducting polymer.[8] Because the energy level of the conduction band of the TiO_2 semiconductor is low (−4.2 eV), large open circuit and low saturation voltages can be achieved using stable, high-work-function electrodes, allowing for improvement in device efficiency, cost, and stability. In order to increase transmission through the top electrode and overall cell performance for the ITO/Ti/TiO_2(NT)/UV-PT/Ag architecture, a thinner layer of Ag can be used (cutting the thickness in half increases the transmission four times). Another possible architecture for backside illumination would be Ti/TiO_2(NT)/UV-PT/ITO, that is, with transparent ITO or fluorine-doped tin oxide (FTO) as the top electrode. These device models are being investigated in ongoing experiments.

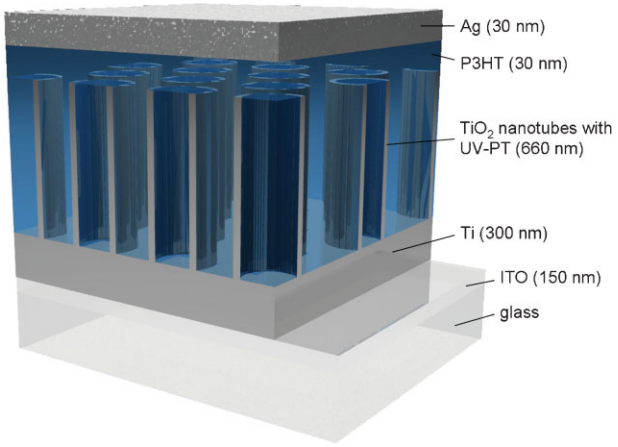

Scheme 1. Schematic of the backside-illuminated heterojunction solid-state solar cell constructed of UV-PT self-assembled onto TiO_2 NT arrays.

In contrast to previously published results on P3HT infiltrated into a mesoporous TiO_2 film[1] in which additional polymer degraded efficiency due to poor hole mobility, we found that solar cell performance increases with an increasing amount of polymer embedded in the TiO_2 NTs (demonstrated later in the paper). In order to maximize the infiltration of the monomer molecules, instead of drop-casting monomer solution onto the TiO_2 NT substrate, we immersed TiO_2 NTs overnight in monomer solution. For P3HT, we found that optimal filling of the TiO_2 NTs was achieved after annealing a film at 225 °C for 15 min on which solution had been drop-cast. Similar results have been reported for a ITO/ZnO nanorod/

NANO MICRO small

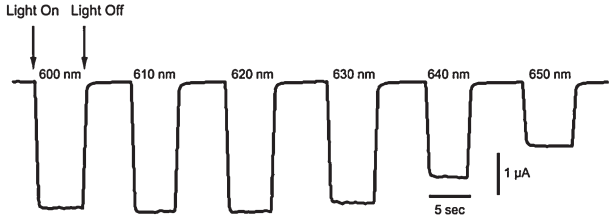

Figure 6. Change in photocurrent upon illumination (light on/light off) in the 600–650-nm range. Maximum change observed around 620 nm. Illumination intensity was the same for each excitation wavelength. Shutter was operated manually leading to the slope visible at each switch event.

P3HT/Ag device, when infiltration of the P3HT into the ZnO nanorod arrays was improved through annealing.[15]

The photoelectrochemical behavior of the ITO/TiO_2 (NT)/UV-PT/Ag device is presented in terms of photocurrent response. Upon illumination with visible light, we observe prompt generation of anodic current (Figure 6). A non-ideal backside-illuminated setup (with an Ag top-electrode optical transmittance of <10%) under illumination of 620-nm light at 38 mW cm^{-2} incident intensity surprisingly yields a photocurrent density as high as 5 μA cm^{-2}. Compared with the reference device infiltrated with pre-synthesized P3HT, the UV-PT cell shows $>10^3$ increase in photocurrent (see Supporting Information). Furthermore, during the light exposure step (light on) in the 600–650-nm range, flat photocurrent values show that charge recombination and space charging during hole transport through the polymer are negligible for the measured timescales. Transient absorption measurements are underway to characterize the behavior at faster timescales. Figure 7 shows photoaction spectra of UV-PT. Since in this backside architecture setup we illuminate the cell through the Ag top electrode, there is a possibility for Ag plasmon-enhanced solar energy conversion. When light is absorbed in the photoactive layer, dipole-allowed photogeneration of excitons scales with the electric field squared. It has been shown that by enhancing the local electromagnetic field with the inclusion of surface-plasmon-active materials, it is possible to enhance the photogeneration of excitons in the polymer.[32] Enhancements to the photogeneration of excitons would lead to higher photocurrents from wavelengths near the plasmon resonance and into the red. Note, however, that in our device when we compare photoaction spectra (Figure 7) and absorption spectra (Figure 5b) of the UV-polymerized device, we can conclude that both vibronic absorption peaks at 580 and 640 nm are photoactive and responsible for the hole transfer process through the polymer (see Supporting Information).

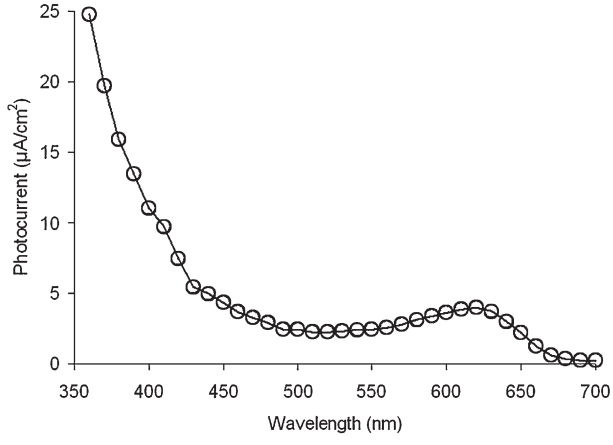

Figure 7. Photocurrent action spectrum of UV-PT recorded in terms of incident photon to generated photocurrent.

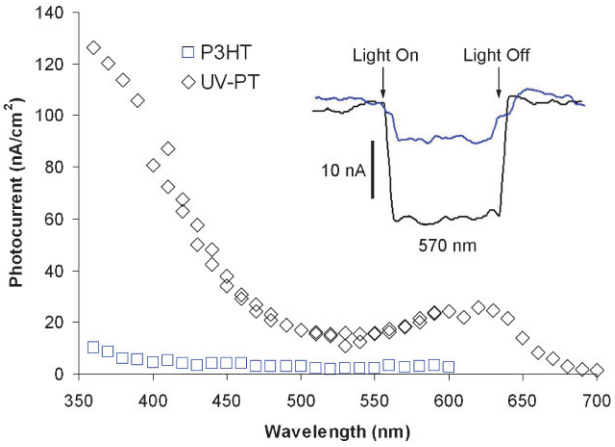

Figure 8. Photocurrent action spectra of UV-PT and P3HT devices recorded in terms of incident photon to generated photocurrent.

In order to investigate the effect of the polymer infiltration technique on device performance, we prepared two films: one by drop-casting DIT monomer precursor solution into TiO_2 NTs followed by UV irradiation (UV-PT) and one by drop-casting pre-synthesized P3HT into TiO_2 NTs. IR absorption spectra were used to confirm that both infiltration techniques resulted in a similar amount of conjugated polymer inside the TiO_2 NTs. When photoaction spectra of these two films are compared (Figure 8) in the region of polymer excitation at 570 nm (Figure 8 inset) we observe as much as a three-fold increase in anodic photocurrent for the UV-PT. Higher crystallinity and better coupling of polymer with the surface of TiO_2 NTs achieved during in situ thin film formation contribute to the observed enhancement. It is also worthwhile to note that the current density in the UV-PT device characterized in Figure 7 is more than 200 times higher than that in Figure 8. The difference between these two samples is the amount of polymer grown inside the titania NTs (greater amount in Figure 7), demonstrating that performance increases with the addition of more polymer as described above.

3. Conclusions

By polymerizing conjugated polymer inside an electron-accepting NT array, we have achieved significant improvements in optoelectronic device performance compared to those fabricated by infiltrating tubes with ex situ synthesized polymer. Our preparation leads to a strong coupling at the

polymer–oxide interface, which is important for efficient exciton separation, and fewer conformational defects, which facilitates hole transport. The small molecule precursor also presumably achieves superior filling within the confined environment. One way to further improve the performance of these organic-inorganic hybrid devices is to optimize photon absorption using a rainbow solar-cell approach.[6] An example would employ TiO_2 NTs packed with an ordered assembly of different-length oligothiophenes. As white light enters the cell, shorter oligothiophenes (larger band gap) will absorb the portion of the incident light with smaller wavelengths. Longer wavelength light, transmitted through the initial layer, will be absorbed by subsequent layers, and so on. By using in situ UV polymerization, a gradient of different length oligothiophenes can be readily created by varying UV exposure time. By constructing an ordered gradient of conjugated oligomers/polymer, it should be possible to increase the effective capture of incident light.

4. Experimental Section

In order to grow vertically oriented TiO_2 NT arrays on conductive transparent electrodes (Scheme 1), the first step is to sputter-deposit a Ti film (≈1-μm thick) on ITO-coated glass. NT arrays of TiO_2 are then formed by potentiostatic anodization of Ti at 15 V in an electrolyte containing 0.27 M NH_4F and 5% deionized H_2O dissolved in formamide as previously described.[33–35] The as-anodized samples are ultrasonically cleaned in deionized water to remove surface debris and subsequently crystallized by annealing in an oxygen atmosphere at 450 °C for 4 h with heating and cooling rates of 1 °C min^{-1}. The morphology of the anodized samples was studied with the use of a JEOL JSM-6300 field emission scanning electron microscope (FESEM). Crystalline TiO_2 NTs were infiltrated with DIT monomer precursor by either drop-casting or overnight immersion in 35 g L^{-1} solution, followed by in situ UV polymerization (ITO/Ti/TiO_2(NT)/UV-PT). For comparison, a reference device was fabricated by infiltrating with P3HT (Sigma–Aldrich, electronics grade, >98% regioregularity) by drop-casting 1 mL of 20 g L^{-1} solution (ITO/Ti/TiO_2(NT)/P3HT). In order to prevent electrons in the TiO_2 from reaching the top silver electrode and short-circuiting the device, a 30-nm overlayer of P3HT was spin-coated on both types of devices. A 30-nm-thick Ag film was sputter-deposited as the top electrode.

The molecular structures of the photochemically synthesized polymers were investigated with ATR-FTIR spectroscopy using a Vertex 70 (Bruker) spectrometer and a 20× ATR objective (Ge-crystal). Optical characterization was carried out with a PerkinElmer LS55 Fluorescence Spectrometer and a PerkinElmer Lambda 950 UV–Vis Spectrometer with a 150-mm integrating sphere. Photoelectrochemical studies were carried out with TiO_2/ITO as the working electrode and Ag as the counter/reference. For spectroelectrochemical measurements a BAS-100B/W (Bioanalytical Systems) workstation was used. The white light source was a 300 W xenon lamp (PerkinElmer). Monochromatic light was provided through a Jobin-Yvon grating monochromator. The density of the incident light (power lamp profile) was measured using a calibrated silicon diode detector (Ophir Optronics); the maximum power of 0.038 W cm^{-2} at 520 nm was measured at the position of the electrodes. All experiments were carried out under ambient conditions.

Acknowledgements

The authors thank D. Rosenmann for help with sputter deposition of Ti and Ag layers and L. Richter for insightful discussions regarding the spectroscopy of conjugated polymers. Use of the Center for Nanoscale Materials was supported by the U.S. Department of Energy, Office of Science, Office of Basic Energy Sciences, under contract no. DE-AC02-06CH11357. This work was also partially funded by the NSF-Materials Research Science and Engineering Center at the University of Chicago.

[1] K. M. Coakley, M. D. McGehee, *Appl. Phys. Lett.* **2003**, *83*, 3380.
[2] A. C. Arango, L. R. Johnson, V. N. Bliznyuk, Z. Schlesinger, S. A. Carter, H.-H. Hörhold, *Adv. Mater.* **2000**, *12*, 1689.
[3] P. A. van Hal, M. P. T. Christiaans, M. M. Wienk, J. M. Kroon, R. A. J. Janssen, *J. Phys. Chem. B* **1999**, *102*, 4352.
[4] T. J. Savenije, J. M. Warman, A. Goossens, *Chem. Phys. Lett.* **1998**, *287*, 148.
[5] M. Grätzel, *Inorg. Chem.* **2005**, *44*, 6841.
[6] A. Kongkanand, K. Tvrdy, K. Takechi, M. Kuno, P. V. Kamat, *J. Am. Chem. Soc.* **2008**, *130*, 4007.
[7] *Organic Photovoltaics: Mechanisms, Materials, and Devices*, Vol. *99*(Eds: S.-S. Sun, N. S. Sariciftci), Taylor & Francis, New York **2005**.
[8] A. C. Arango, S. A. Carter, P. J. Brock, *Appl. Phys. Lett.* **1999**, *74*, 1698.
[9] K. Shankar, G. K. Mor, H. E. Prakasam, O. K. Varghese, C. A. Grimes, *Langmuir* **2007**, *23*, 12445.
[10] K. Zhu, N. R. Neale, A. Miedaner, A. J. Frank, *Nano Lett.* **2007**, *7*, 69.
[11] K. Shankar, G. K. Mor, M. Paulose, O. K. Varghese, C. A. Grimes, *J. Non-Cryst. Solids* **2008**, *354*, 2767.
[12] M. Paulose, K. Shankar, O. K. Varghese, G. K. Mor, C. A. Grimes, *J. Phys. D* **2006**, *39*, 2498.
[13] C. Goh, K. M. Coakley, M. D. McGehee, *Nano Lett.* **2005**, *5*, 1545.
[14] K. M. Coakley, Y. Liu, M. D. McGehee, K. L. Frindell, G. D. Stucky, *Adv. Funct. Mater.* **2003**, *13*, 301.
[15] D. C. Olson, Y.-J. Lee, M. S. White, N. Kopidakis, S. E. Shaheen, D. S. Ginley, J. A. Voigt, J. W. P. Hsu, *J. Phys. Chem. C* **2007**, *111*, 16640.
[16] C.-W. Hsu, L. Y. Wang, W.-F. Su, *J. Colloid Interface Sci.* **2009**, *329*, 182.
[17] W. J. E. Beek, M. M. Wienk, M. Kemerink, X. Yang, R. A. J. Janssen, *J. Phys. Chem. B* **2005**, *108*, 9505.
[18] G. Liu, S. Natarajan, S. H. Kim, *Surf. Sci.* **2005**, *592*, L305.
[19] S. Natarajan, S. H. Kim, *Thin Solid Films* **2006**, *496*, 606.
[20] S. H. Kim, S. Natarajan, G. Liu, *Catal. Today* **2007**, *123*, 104.
[21] S. V. Babu, M. David, R. C. Patel, *Appl. Opt.* **1991**, *30*, 839.
[22] D. Mardare, P. Hones, *Mater. Sci. Eng.* **1999**, *68*, 42.
[23] S. B. Darling, *J. Phys. Chem. B* **2008**, *112*, 8891.
[24] S. B. Darling, M. Sternberg, *J. Phys. Chem. B* **2009**, in press.
[25] Y. Zhang, C. Wang, L. Rothberg, M.-K. Ng, *J. Mater. Chem.* **2006**, *16*, 3721.
[26] C. L. Huisman, A. Huijser, H. Donker, J. Schoonman, A. Goossens, *Macromolecules* **2004**, *37*, 5557.

[27] K. Tashiro, M. Kobayashi, T. Kawai, K. Yoshino, *Polymer* **1997**, *38*, 2867.
[28] P. M. Kumar, S. Badrinarayanan, M. Sastry, *Thin Solid Films* **2000**, *358*, 122.
[29] R. Colditz, D. Grebner, M. Helbig, S. Rentsch, *Chem. Phys.* **1995**, *201*, 309.
[30] L. Li, G. Lu, X. Yang, *J. Mater. Chem.* **2008**, *18*, 1984.
[31] D. R. Sahu, J.-L. Huang, *Thin Solid Films* **2006**, *515*, 876.
[32] A. J. Morfa, K. L. Rowlen, I. T. H. Reilly, M. J. Romero, J. van de Lagemaat, *Appl. Phys. Lett.* **2008**, *92*, 013504.
[33] M. Paulose, K. Shankar, S. Yoriya, H. E. Prakasam, O. K. Varghese, G. K. Mor, T. A. Latempa, A. Fitzgerald, C. A. Grimes, *J. Phys. Chem. B* **2006**, *110*, 16179.
[34] K. Shankar, G. K. Mor, A. Fitzgerald, C. A. Grimes, *J. Phys. Chem. C* **2007**, *111*, 21.
[35] H. E. Prakasam, K. Shankar, M. Paulose, O. K. Varghese, C. A. Grimes, *J. Phys. Chem. C* **2007**, *111*, 7235.

Received: January 15, 2009
Published online: April 14, 2009

